THE JOURNAL OF PHYSICAL CHEMISTRY B

Article

pubs.acs.org/JPCB

Thermodynamic Study on Dynamic Water Vapor Sorption in Sylgard-184

Stephen J. Harley,* Elizabeth A. Glascoe, and Robert S. Maxwell

Physical and Life Sciences Directorate, Lawrence Livermore National Laboratory, 7000 East Avenue, Livermore, California 94550-9698, United States

Supporting Information

ABSTRACT: The dynamic and equilibrium water vapor sorption properties of Sylgard-184, a commercially available poly(dimethylsiloxane) elastomer (PDMS), were determined via gravimetric analysis from 30 to 70 °C. Described here is a methodology for quantitatively assessing how water vapor diffuses and ad/absorbs into polymeric materials that are traditionally considered hydrophobic. PDMS materials are frequently chosen for their moisture barrier properties; our results, however, demonstrate that moisture is able to penetrate the material over a range of temperatures and humidities. The sorption values measured here ranged from ca. 0.1 to 1.4 cm^3 (STP) H_2O/g Sylgard. The isotherms exhibited sigmoidal character and were fit to a triple mode sorption model. Asymptotic behavior at low water activities was characterized using a Langmuir type adsorption model, linear behavior was fit to a Henry's law type dependence, and the convex portion at higher activities was fit with good agreement to Park's equation for pooling or clustering. The thermal dependence of these sorption modes was also explored and reported. The dynamics of the sorption process were fit to a Fickian model and effective diffusivities are reported along with corresponding activation energies. The diffusivity values measured here ranged from ca. 0.5 to 3.5 × 10^{-5} cm^2/s depending on the temperature and relative humidity. The concentration dependence of the diffusivity showed a direct correlation with the three modes of uptake obtained from the isotherms. Corrections to the diffusivities were calculated using existing models that take into account adsorption and pooling.

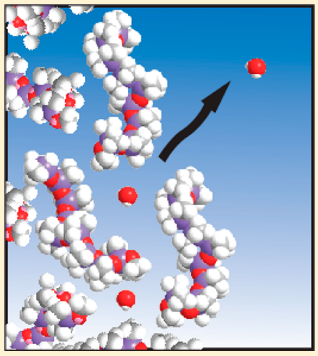

INTRODUCTION

Poly(dimethylsiloxane) (PDMS)-based materials are used in a wide range of applications because they are nontoxic, relatively inert, easy to fabricate, and have favorable optical and mechanical properties. In addition, the high dielectric strength coupled with the ease of casting PDMS around arbitrary shapes makes it ideal for encapsulating sensitive electronic circuitry.[1] PDMS materials are widely regarded as hydrophobic, consequently they are used as moisture barriers in photovoltaic cells[2,3] and as fluid channels in microfluidic devices.[4−7] In spite of the hydrophobic nature of the PDMS, water vapor still has the ability to sorb and diffuse through PDMS at, albeit, an attenuated rate. Over time, water intrusion through the PDMS layer and into an electronic device could result in corrosion, shorting, and other types of electronic failure. As such, accurate knowledge of the dynamic sorption processes may lead to a better determination of aging and or failure predictions of devices.

There is extensive literature on moisture diffusion rates and mechanisms in PDMS systems.[8−10] The reported rates of diffusion vary considerably, in spite of the fact that these were ideal networks having exclusively $(Si(CH_3)_2-O)_n$-based moieties. Baron showed that this variability results from trace impurities within the networks, specifically hydroxyl functional groups.[11] These impurities, while too dilute to have an effect on mechanical properties, can cause substantial variation in the expected dynamic sorptive behavior of PDMS networks. Moreover, commercial blends of PDMS often incorporate significant stoichiometric excesses of reactive functional groups, processing aids, and filler materials in order to modify mechanical properties and optimize the curing behavior.[12,13] For example, in Sylgard-184 high surface area silica is added to enhance the tear strength and elongation properties; however, in doing so, high density hydroxyl groups inherent to the silica will alter the materials permeation properties.[11] Thus, it becomes impossible to blanket dynamic sorption properties under one name (i.e., PDMS); rather each formulation will need to be independently analyzed.

Here we investigated the sorption and diffusion of moisture through Sylgard-184 over a wide range of temperatures and relative humidities (RH) in order characterize and quantify the mechanisms of moisture uptake and transport through the material. The formulation chemistry in Sylgard-184 was intentionally designed with a stoichoimetrically large excess of silane groups in order to achieve a complete cure of the system over a reasonable time-scale at room temperature. These groups readily hydrolyze upon exposure to moisture resulting in hydroxyl groups within the material and outgassing of hydrogen gas. Our samples were pretreated with moisture in order to fully react and hydrolyze all of the available Si−H

Received: June 18, 2012
Revised: November 13, 2012
Published: November 15, 2012

groups; consequently, our material has more hydroxyl groups than a pristine sample. Kempe reported diffusivities for Sylgard-184 at four different temperatures;[2] Kempe's measurements were suitable for the purposes of their study but lacked the extensive sorption and variable diffusion parameters reported herein. In addition, Kempe does not discuss sample pretreatment, so the state of the material and the concentration of silane groups are unknown. Our results indicate that the sorption and diffusion properties and mechanisms of Sylgard-184 are dependent on both the temperature and relative humidity. These results can be directly utilized in evaluating the moisture egress rates into photovoltaic cells and other electronic devices, microfluidic devices, sealants, and for a variety of other applications. More importantly, the approach and methodology discussed here can be applied to a variety of different polymeric materials in order to characterize and quantify the subtle behaviors of moisture in hydrophobic materials.

EXPERIMENTAL SECTION

Materials and Sample Preparation. Sylgard-184 samples were prepared using a kit obtained from Dow Corning. The kit is a two-part resin/curing agent consisting of vinyl end-capped oligomeric dimethyl siloxane chains cross-linked with methyl hydrosiloxane reinforced with trimethylated silica, and a platinum catalyst. There are likely additional chemicals in the two-part resin/curing agent kit; however, because Sylgard-184 is a commercial and proprietary formulation, only the major constituents are listed.

A 10:1 volume ratio of resin to curing agent was mixed using a FlackTec speed mixer DAC 150 FVZ and then cast into high-density polyethylene rectangular molds having a geometry of 2″ × 6″ × 0.08″. Trapped air bubbles, which were introduced during mixing, were removed by placing the molds in a vacuum for approximately 10 min. The samples were cured at 25 °C for 12 h and then further dried in vacuum for 24 h to remove residual volatiles.

The fully cured samples were removed from their molds and cut into a strip 3.8 cm ×7.6 cm × 0.2 cm thick, which was previously determined to be the optimum sample size for the IGAsorp. During preconditioning, the samples were exposed for 6 days to a 400 mL/min stream of 50 °C nitrogen gas with a relative humidity of 50%. The sample mass loss was monitored over this time and observed to stabilize on the fifth day, with no further changes into the sixth day. Mass spectrometry measurements of the outgassing species observed during this 6 day period included H_2 (a product of silane hydrolysis), and larger molecular weight species that we were unable to identify. Further work is underway to characterize these outgassing species and the formation mechanisms.

Preceding each sorption isotherm, samples were exposed to a dry nitrogen stream for 12 h to ensure the material was void of water. This allows for the 0% RH data point to be truly representative of a dry sample.

Dynamic Sorption. The dynamic water vapor sorption isotherms were acquired using an IGAsorp developed by Hiden Isochema. This instrument consists of a fully automated microbalance (0.1 μg sensitivity) in a thermally controlled chamber equipped with a vapor generator, which allows for the setting of discrete relative humidity values within the chamber. By flowing moisture-charged carrier gas through the chamber (typically N_2 for our application) and gently heating the sample, the sorption process is quantified via sample mass changes. A quadruple mass spectrometer (HPR-20 by Hiden Analytical) with a heated capillary is attached to the effluent stream of the IGAsorp to monitor for signs of material outgassing and degradation during the sorption process.

Isotherms were acquired in steps of 5% RH where a sample was considered to be in equilibrium with the vapor stream upon reaching 98% of the predicted equilibrium mass uptake. A simple asymptotic rise to equilibrium was used for this forward prediction. Figure 1 shows a sample data set with chamber humidity and sample mass changes.

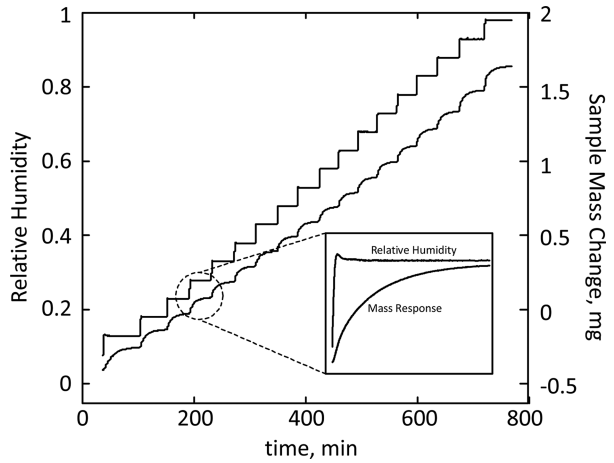

Figure 1. Relative humidity steps with the corresponding mass response for Sylgard-184 at 30 °C in the IGAsorp.

Isotherms were collected at 30, 40, 50, 60, and 70 °C; at each temperature, both a sorption isotherm and a desorption isotherm were collected back to back. There was no evidence of hysteresis. Further, upon completing the temperature series, the 40 °C was rerun to check for sample response continuity. The results matched the prior 40 °C run within experimental error.

RESULTS AND DISCUSSION

Sorption. The sorption isotherm data for Sylgard-184 at 30 and 70 °C are shown in Figure 2; isotherms at 40, 50, and 60 °C (not shown) have the same general trend. Sylgard-184 is a rubbery elastomer that is homogeneous on the macroscopic level yet it contains discrete regions with variable chemical and structural properties at the microscopic level. Not surprisingly, the isotherms in Figure 2 have a complex, nonlinear shape indicative of multiple mechanisms of moisture sorption.

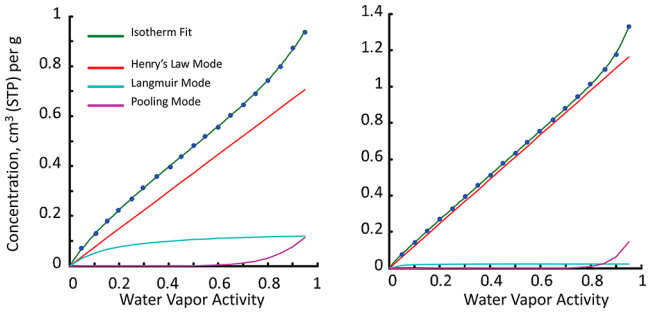

Figure 2. Experimentally measured moisture isotherms (dots) and trimodal fit (eq 2) at 30 °C (left) and 70 °C (right). The contribution of each mode is also plotted.

dx.doi.org/10.1021/jp305997f | J. Phys. Chem. B 2012, 116, 14183−14190

The simplest model for the solubility of a gas into a polymeric material is a Henry's law absorption model:[14]

$$C = k_D p \quad (1)$$

where C is the gas concentration in the material, k_D is the Henry's law solubility coefficient, and p is the partial pressure. While Henry's law absorption is traditionally applied to gaseous absorption in a liquid, Sylgard-184 is a cross-linked polymer with a glass transition temperature of −122.6 °C;[15] at the temperatures studied here, it can be thought of as a constrained liquid. This is to say that the free space that allows for liquid-like chain motions can be occupied by gas phase water molecules via a noninteracting dissolution-based phenomenon. The ability for water vapor to enter this mode is strictly statistical in nature. In other words, an increase in the number of external water vapor molecules increases the probability of entering a free volume of some proportional amount (i.e., kD). Unlike glassy polymers, which have static voids, the voids in Sylgard-184 are expected to be dynamic, resulting in a dynamic statistical distribution of free volume as dictated by intersegmental chain motions. The mobility of Henry's law water molecules is limited by the movement of these chain motions thereby impeding bulk water mobility.

This simple, linear model is unable to account for the prominent nonlinear sorption properties seen in Sylgard-184, particularly at the lowest and highest vapor activities. Hydrophilic regions in the material allow for immobilization of water molecules via a Langmuir type adsorption.[16,17] There is some debate as to the true source of water immobilization in strictly hydrophobic systems,[11] however, in Sylgard-184, the most likely sites for Langmuir adsorption are the silica filler and Si−OH groups that were formed via hydrolysis of excess silane. Langmuir adsorption will manifest in the isotherm as an asymptotic rise to equilibrium at small values of water vapor activity. At higher activities in Figure 2, the drastic increase in solubility is attributed to the aggregation, clustering, or pooling of water molecules that presumably grow from the Langmuir sites.[18] A model for this process was developed by Park,[19] which is based off the equilibrium between free and pooled water.

A more comprehensive mathematical description of the sorption process is a sum of the three contributions:

$$C = C_{Henry} + C_L + C_P = k_D p + \frac{C'_H b p}{1 + bp} + \frac{K'_c (k_D p_{sat})^n p^n}{n} \quad (2)$$

where C is the total gas concentration (cm^3 STP g^{-1}), C_{Henry} is the concentration from Henry's mode (cm^3 STP g^{-1}), C_L is the concentration from the Langmuir mode (cm^3 STP g^{-1}), C_P is the concentration from the pooling mode (cm^3 STP g^{-1}), C'_H is the Langmuir capacity constant (cm^3 STP g^{-1}), b is the Langmuir affinity constant (cm Hg^{1-}), K'_c is the equilibrium constant for the clustering reaction, p_{sat} is the saturation pressure (cm Hg^{1-}), and n is the mean number of water molecules per cluster. A convenient way to compare isotherms from different temperatures is to re-express eq 2 in terms of water activity, defined as $a = p/p_{sat}$. This equation along with the fitted parameters may be found in the Supporting Information.

Figure 2 shows the results of utilizing eq 2 to deconvolve the contribution of each sorption mode from the experimental data. One should note that these results reflect the equilibrium state at each relative humidity step; dynamics such as diffusion rates are discussed in a subsequent section. The results upon the application of eq 2 to the isotherms are listed in Table 1. It is evident from the results in Figure 2 that the main contribution to sorption of moisture in Sylgard-184 is via absorption (i.e., Henry's law mode; linear curve in Figure 2). Yet one can see at low moisture levels that the adsorption of moisture (i.e., Langmuir contribution, asymptotic curve in Figure 2) can be important, and, at high moisture levels, the pooling or clustering of water dominates (i.e., exponential rise in Figure 2). The mechanism for moisture pooling at elevated humidities is not understood.

Table 1. Sorption Parameters Resulting from the Fit of the Experimental Data to Eq 2

temperature (°C)	k_D (cm^3 STP g^{-1})	C'_H (cm^3 STP g^{-1})	b (cm Hg^{1-})	log K'_C	n (molecules per cluster)
30	0.234	0.142	1.83	−12.2	7.7
40	0.162	0.057	2.48	−14.7	11.3
50	0.113	0.037	2.82	−16.5	14.1
60	0.082	0.024	2.51	−17.5	15.8
70	0.062	0.012	9[a]	−17.1	16.2

[a]The 70 °C run did not display sufficient Langmuir behavior to report reliable parameters.

Table 2. Arrhenius Parameters for b, k_D, and C'_H

Henry's Law Solubility	
ΔH_{k_D} (kJ/mol)	−28.88
k_{D0} (cm^3 STP g^{-1} $cmHg^{-1}$)	2.35×10^{-6}
Affinity for Langmuir Sites	
ΔH_b (kJ/mol)	25.51
b_0 ($cmHg^{-1}$)	4.4×10^4
Capacity of Langmuir Sites	
$\Delta H_{C'_H}$ (kJ/mol)	−50.20
C'_{H0} (cm^3 STP g^{-1})	2.86×10^{-10}
Temperature for $C'_{H0} = 0$	
T (°C)	79

The thermal dependence of the Henry and Langmuir sorption parameters in Table 2 (i.e., b and k_D) were fit to a van't Hoff-type temperature dependence:

$$\text{parameter} = A_{r0} e^{-\left(\frac{\Delta H}{RT}\right)} \quad (3)$$

where R is the ideal gas constant, T is the absolute temperature, the prefactor A_{r0} is represented as b_0 and k_{D0} with respect to the germane parameter, and ΔH_b and ΔH_{k_D} are the enthalpies of solution for the Henry mode and Langmuir mode respectively. The Langmuir capacity constant (i.e., C'_H) was also fit to this Arrhenius dependence; the prefactor and enthalpy are represented by C'_{H0} and $\Delta H_{C'_H}$. The physical meaning of the Langmuir capacity Arrhenius dependence is not clear;[20] rather, we report these values as "apparent" parameters. All of the Arrhenius parameters are reported in Table 2.

The Henry's law contribution to water sorption is the dominant mode of uptake in Sylgard-184. The negative enthalpy indicates a diminishing contribution of this mode with increasing temperature; however, the nearly 2-fold larger

dx.doi.org/10.1021/jp305997f | J. Phys. Chem. B 2012, 116, 14183−14190

enthalpy for the Langmuir capacity results in the Henry's mode always dominating the uptake. It should be noted that even at the highest possible uptake activity and temperature, water comprises only 0.1% of the total mass (on a mass to mass basis).

Figure 3 shows the concentration of water molecules that are surface adsorbed via the Langmuir mode (i.e., C_L) as a function

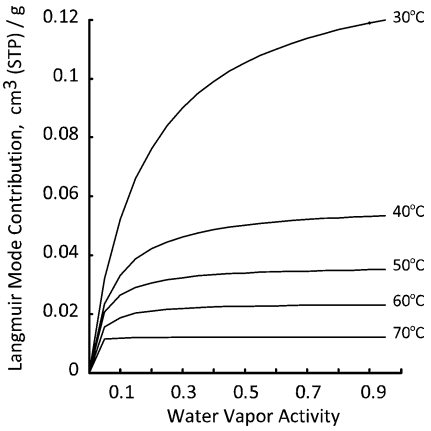

Figure 3. Thermal dependence of the Langmuir mode (C_L).

of moisture content (i.e., vapor activity) at five different temperatures. The Langmuir capacity constant is the maximum number of sites available for water adsorption and corresponds to the asymptote value for each curve. It is clear that the Langmuir capacity constant decreases with increasing temperature, where, upon linear extrapolation, it should reach a null contribution at 79 °C. Previous studies on elastomers indicate a similar trend where the Langmuir capacity decreases with increasing temperature.[21] This temperature dependence is logical if one thinks about the physical mechanism of a water molecule sticking to the elastomer surface via a hydrogen bond. As the temperature increases, the water molecules have greater kT energy, which effectively lowers the barrier to breaking the hydrogen bond; thus one would expect the equilibrium to shift away from Langmuir-type adsorption.

The Langmuir affinity constant (i.e., b), which is calculated from the data in Figure 3, increases with temperature. b is defined as the ratio between the adsorption and desorption rate constants, i.e., $b = k_{ads}/k_{des.}$ A positive correlation between temperature and b could either mean that the adsorption rate increases with temperature or the desorption rate decreases with temperature. Each scenario is logical if one thinks about the underlying changes in collisional frequency and activation energies of the water molecules as temperature changes. In the collisional frequency argument, as temperature increases, the kinetic theory of gases postulates that each molecule is likely to collide with the polymer surface more frequently, hence the probability of a water molecule locating a Langmuir site increases with temperature. If water molecules are finding the Langmuir sites more quickly when heated, it is plausible that the adsorption rate (k_{ads}) will increase. In the activation energy argument, the kinetic theory of gases postulates that, as temperature increases, the kinetic energy of each gas-phase water molecule will increase. Therefore, if the water molecule forms a weak attachment with a Langmuir site, raising the temperature may reduce the total number of Langmuir sites because the weakest sites have been eliminated (i.e., the water molecule may simply not stick to these weak sites because the internal energy pops it off again). In this scenario, only Langmuir sites with a stronger affinity for water would be able to capture water molecules, and the desorption rates from these strong interactions will slow. If one thinks of the material as having a distribution of different Langmuir binding sites with a distribution of different affinities, eliminating the weakest sites will shift the population to just the stronger binding sites, and hence the global desorption rate may appear to decrease. Thus raising the temperature may eliminate the weak binding sites, and the global rate of desorption (k_{des}) could decrease. Keeping in mind that Sylgard-184 is a heterogeneous material, we hypothesize that there are a multiple different types of Langmuir sites with different binding energies for water. For example, the silica particles in Sylgard-184 are expected to have both hydrophobic regions due to the surface-modified coupling agent (i.e., trimethyl or dimethylated) and hydrophilic regions, and silanol groups in Sylgard-184 are expected to have a relatively weak affinity for water, especially at elevated temperatures. Hence, with both the collisional frequency and activation energy arguments, it is logical that the Langmuir affinity constant increases with temperature.

At activities greater than approximately 0.7, the clustering or pooling phenomena becomes important. The positive correlation between the number of water molecules in each cluster (i.e., n) and temperature (see Table 1) may indicate thermal expansion of void spaces within the polymer at higher temperatures. However, the certainty toward the exact number of water molecules per cluster is hindered by the small sensitivity of n toward the uptake. This is to say that small variations in n do not have a large effect on the contribution of the pooling mode. This same small sensitivity is also seen in K'_C where, for example, in Table 1, a positive temperature correlation is observed, yet K'_C should be independent of temperature. Attempts were made to use other models to fit this high activity region, such as the BET type II model; however, they never fit as well as eq 2.

Diffusion. The diffusivity of moisture in Sylgard-184 was determined based on our experimental sorption kinetics and established diffusivity models. The diffusive flux of moisture out of the material may be modeled with Fick's law:

$$J = -D\Delta C \tag{4}$$

where conservation of mass allows one to invoke the continuity equation:

$$\frac{\partial C}{\partial t} = -\nabla J \tag{5}$$

where J is the diffusive flux, D is the diffusivity, C is the concentration, and t is time. By ignoring edge effects, the rectangular symmetry of the Sylgard sample used in these experiments allows for the reduction of the flux and continuity equations to a single dimension. Upon combining the two equations, one arrives at the familiar form of Fick's second law:

$$\frac{\partial C(x,\,t)}{\partial t} = -D\frac{\partial^2 C(x,\,t)}{\partial x^2} \tag{6}$$

where x is position, in our case depth. It should be noted that the diffusivity was assumed to be independent of position, an assumption we deem to be valid as long as the partial pressure steps chosen remain small. However, the assumption that the diffusivity is constant across the entire desorption process is invalid, as will be demonstrated below.

At a nitrogen flow rate of 250 mL/min within the IGAsorp, it is also assumed that all the water effluent from the surface of the material is immediately removed from the surface such that a constant concentration boundary condition would apply. In other words, there is no mass boundary layer impeding the outgassing process, and the flux is due to diffusion internal to the part. A boundary layer impedance will manifest as sigmoidal behavior in the early time points of the mass loss versus $\sqrt{t}$ plot; such behavior was seen at low flow rates but not at 250 mL/min.

If the concentration is uniform at time zero, Crank[22] has found a solution of the following form:

$$\frac{M(t)}{M_\infty} = 1 - \frac{8}{\pi^2}\sum_{n=0}^{\infty} \exp\left(\frac{-D(2n+1)^2\pi^2 t}{l^2}\right) \tag{7}$$

where $M(t)$ is the mass gain at time t, M_∞ is the mass gain at infinite time, and l is the thickness of the sample. This is a simple model for determining diffusivity that is widely used by researchers; however, the model does not appear to be sufficient for our analysis of Sylgard-184, as will be discussed below.

The results for the regression of the experimental data to eq 7 are depicted in Figure 4. In systems with Henry mode-only

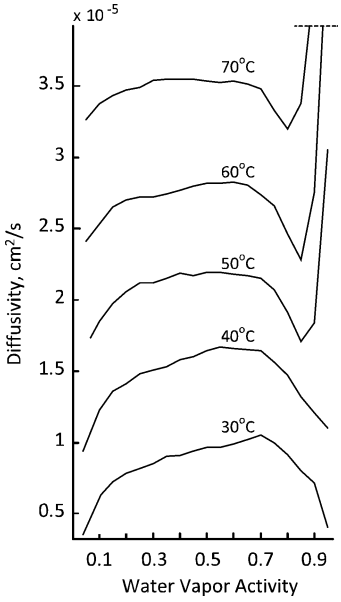

Figure 4. Diffusivity as a function of water vapor activity at five different temperatures.

absorptive character, a constant or flat diffusivity profile is expected.[23] The shapes of the diffusivity curves in Figure 4 are not flat, especially at the lower temperatures. This indicates that moisture diffusion in Sylgard-184 is dictated by more complex mechanisms than just the water absorbed via Henry's law. At all the measured temperatures, the diffusivity rises at the lower water activities, which correlates with the Langmuir contribution to the sorption (see Figure 5). The drop in diffusivity at elevated vapor activities correlates with the rise in the pooling contribution to sorption (see Figure 5).

The diffusion model shown in eq 7 ignores the moisture contributions from Langmuir and pooling sites within the material and a more sophisticated model is necessary to separate out these contributions. In eq 7, the concentration gradient for moisture ($\delta C/\delta x$) has been oversimplified. In our simplified application of classical Fick's law, the flux is proportional to the total concentration gradient scaled by a diffusion constant:

$$J = -D\frac{\partial C}{\partial x} \sim D\frac{\Delta C}{\Delta x} \tag{8}$$

Here the concentration gradient is just the difference between the outside partial pressure and internal concentration, which is the sum of the three modes:

$$\Delta C = p_{H_2O} - (C_{Langmuir} + C_{Henry} + C_{Pooling}) \tag{9}$$

However, the population of mobile water molecules will obey Henry's law[24] and some small fraction of the Langmuir mode;[25] the remaining population of water in the material is immobile and therefore not part of the true chemical potential difference driving the species migration:

$$\Delta C = p_{H_2O} - (C_{Henry} + X \times C_{Langmuir}) \tag{10}$$

where X is the fraction of the Langmuir mode that is mobile. At first, water is immobilized on surface sites and the concentration in the bracketed term of eq 10 will not increase with increasing water partial pressures, thereby skewing the ΔC ever greater for each step. In the derivation of eq 7, we do not take this water immobilization process into account; this skewing of the concentration gradient will manifest as an increase in observed diffusivity.

For example, if a completely dehydrated sample is exposed to a moisture step from 0 to 5% RH, most of the water will adsorb and immobilize at sites in the polymer via the Langmuir mode with little in the Henry's mode. In this situation, the relative humidity or concentration of mobile water molecules at the surface is 5%, but in the interior it is 0%. If the partial pressure is increased to 10% RH, again most of the water is adsorbed via Langmuir mode, and the concentration of mobile water molecules is 10% at the surface and 0% in the interior. Because we measure the flux in eq 8, the experimental diffusivity must skew to compensate for the unaccounted change in concentration gradient, hence the changing diffusivity as a function of RH. All numbers were hypothetical and hyperbolized in this example. A mathematical model was proposed by Paul and Koros[25] where they include the effect of partial immobilization of water caused by the Langmuir mode:

$$D_{exp} = D_m\left(\frac{1 + \frac{FK}{(1+\alpha C_H)^2}}{1 + \frac{K}{(1+\alpha C_H)^2}}\right) \tag{11}$$

where D_m is the diffusivity of the mobile species, F is the fraction of the Langmuir mode associated with mobility. $K = (C'_H b)/k_D$ and $\alpha = b/k_D$ are constants derived from the sorption isotherm. Only our 30 and 40 °C data could be analyzed with eq 11 because the Langmuir contribution at higher temperatures was so limited that there was insufficient data for a reliable fit. Using eq 11, we were able to calculate a constant diffusivity over a wide range of vapor activities and eliminate the skew introduced by the Langmuir sorption effects. Diffusivity values for activities below 0.05 and above 0.9 drastically reduced the certainty for the fit to eq 11; they were considered outliers and were omitted from the regression. A comparison of the fit using eq 11 with the diffusivity data at 30 °C is shown in Figure 5 (right), and the results are summarized

dx.doi.org/10.1021/jp305997f | J. Phys. Chem. B 2012, 116, 14183−14190

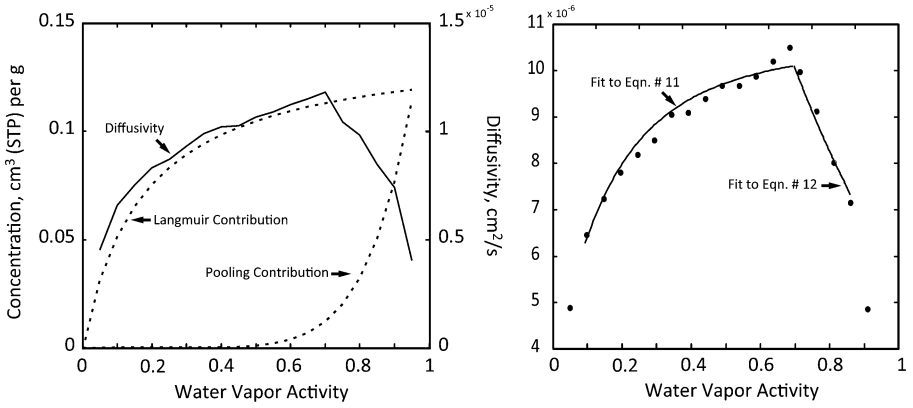

Figure 5. Comparison of the diffusivity curve at 30 °C to the Langmuir (C_L) and pooling (C_P) sorption curves (left) and plot of experimental diffusivity data fit to eq 11 and 12 (right). Note the diffusivity axes have different scales.

Table 3. Results of the Regression of the Diffusivity Data to Eqs 11 and (12)

temperature (°C)	D_m (cm^2 s^{-1})	F	β (cm^2 STP)
30	1.12×10^{-5}	2.2×10^{-10}	−0.251
40	1.65×10^{-5}	1.14×10^{-9}	−0.386

in Table 3. The very small value for F indicates that the fraction of Langmuir sites that are mobile are negligible (although these Langmuir bound water molecules will still attenuate the diffusivity of the mobile water via weak hydrogen bonding), and thus when talking about the concentration of mobile sites for this system, the use of C_{Henry} is appropriate.

In the Henry region, the diffusivity is essentially constant. This is most evident in the 70 °C run where the Langmuir mode is minor compared to the Henry's law mode (see Figure 2). However, when the internal voids of which Henry's law species occupy increase further, the collisional frequency between adjacent waters will become more prominent than the collisions with the polymer matrix. This will lower the mean free path for water and manifest as a drop in diffusivity (see Figure 5).

In order to account for this drop in diffusivity at elevated water activities, i.e., where pooling becomes a factor, a different model was used. The steric effects of clustering water were investigated by Stern[20] who developed a phenomenological model for the reduction in diffusivity:

$$D_{exp} = D_{m0} \exp(\beta(C_m - C_{m0}))\frac{dC_m}{dC} \quad (12)$$

where β is the rate constant for concentration-dependent diffusivity, C_m is the concentration of the mobile species, D_{m0} is the diffusion coefficient of the mobile species for $C_m = C_{m0}$, and the term dC_m/dC was calculated from the sorption isotherms. Visual inspection of the diffusivity plots at 30 and 40 °C (see Figure 4) indicates that pooling begins to occur at a vapor activity of approximately 0.7. Consequently, the value for C_{m0}, i.e., the initial water concentration before pooling comes into play, was extracted from the isotherm data at a vapor activity of $a = 0.7$. The very small contribution of Langmuir sites to mobile sites allow for C_m to be replaced by C_{Henry}. Using this model, the diffusivity data at 30 and 40 °C were fit at the higher vapor activities (i.e., $a > 0.7$) in order to determine the validity of this model to our system and to extract a value for β. A comparison of the fit to the diffusivity data is shown in Figure 5 (right), and the values for β are listed in Table 3. Diffusivity values for activities below 0.05 and above 0.9 reduced the certainty for the fit to eq 12 and were omitted from the regression.

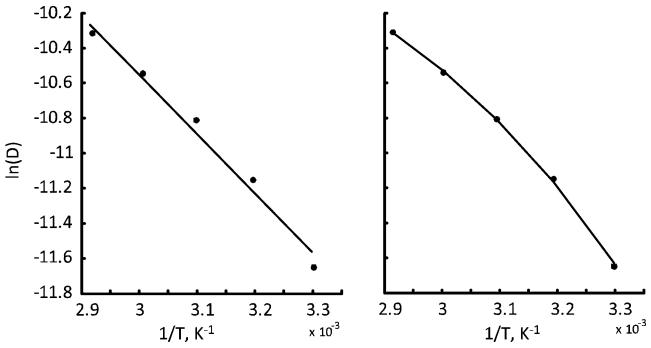

Figure 6. Arrhenius plots of the diffusivity at a water activity of 20% fitting to the standard Arrhenius equation, left, and to the stretched Arrhenius equation (eq 13), right.

At higher temperatures and large vapor activities, the diffusivity drastically increases, while at lower temperatures it drops just as predicted by eq 12. Presumably, this sharp increase is due to the material changing volume (plasticization) under the stress of the higher temperature and pooling effects. The expansion of the material would lead to a larger mean free path and thus a larger diffusivity. Further investigation is needed to be certain. It is important to note that this material expansion was completely reversible, as no hysteresis was observed in the isotherms.

The thermal dependence of the uncorrected diffusivity does not universally fit an Arrhenius-type model as one would expect.[26] This is most true at partial pressures where Langmuir or pooling are active in the isotherm, which again is due to the diffusion model not incorporating the effects of Langmuir immobilization and clustering. While we were able to retrospectively account for these effects at 30 and 40 °C, we were unable to do so at the higher temperatures. Thus, in an attempt to obtain activation energies for the diffusion process, the uncorrected diffusivities were fit to a stretched form of the Arrhenius equation:

$$D = Ae^{-\left(\frac{E}{RT}\right)^{\gamma}} \quad (13)$$

where E is the activation energy, A is the Arrhenius prefactor, T is the temperature, R is the ideal gas constant, and γ is the

dx.doi.org/10.1021/jp305997f | J. Phys. Chem. B 2012, 116, 14183−14190

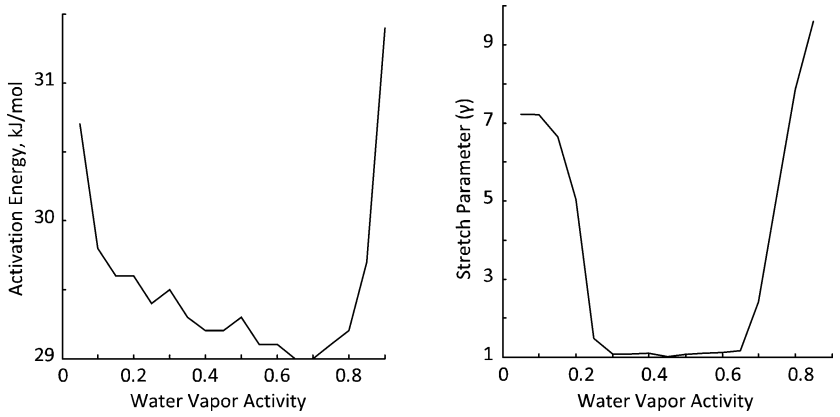

Figure 7. Arrhenius parameters dependence on water vapor activity.

stretched parameter that is indicative of the deviation from exponential behavior.[27]

Figure 6 shows both a fit using the standard Arrhenius model and a stretched model (eq (13). It is clear that the Arrhenius fit is fine, but the stretched Arrhenius model fits the data much better. As seen in Figure 7, in the lower activity region, the activation energy drops from 30.7 kJ/mol to approximately 29.3 kJ/mol at an activity of 0.3. The energy then remains moderately constant from 0.3 until 0.7 slowly, yet systematically, dropping to 29.0 kJ/mol. At 0.7 when the clustering starts to dominate, the energy jumps to 31.4 kJ/mol at an activity of 0.9. The results for each activity may be found in the Supporting Information.

This same trend is also seen in the stretched parameter, γ, where deviations from true Arrhenius behavior ($\gamma > 1$) occur in the same Langmuir and pooling dominated activities. However, when these modes are not active, a traditional Arrhenius model ($\gamma = 1$) fits very well.

CONCLUSIONS

The sorption and diffusion of moisture into PDMS materials is an important topic because of the popularity of the materials in a wide range of applications and the susceptibility of many of these devices to moisture. Due to the presence of native excesses in reactive functional groups, residual small molecule byproducts from resin synthesis/curing, fillers, and processing aids, the behavior of moisture in PDMS networks can vary considerably. Here we have characterized and quantified the sorption and diffusion of moisture through Sylgard-184, a commercially available PDMS material that is widely used and is particularly popular as a protection layer in photovoltaic cells. Our study spans a wide range of moisture levels and temperatures in order to explore the relevant conditions where this material may be used. Our results indicate that both sorption and diffusion depend heavily on the temperature and relative humidity. Under most conditions, Sylgard-184 behaves like an idealized PDMS network where moisture sorption obeys Henry's law. However, at low relative humidities, Sylgard-184 adsorbs a small but significant amount of water, obeying Langmuir's model, and at high humidity, it is clear that moisture begins to aggregate or pool in the material. These various modes of sorption affect the diffusivity of moisture through the material, and several models were utilized to accurately describe the data. Our results for diffusivity are the same order of magnitude as results presented previously by Kempe,[2] however, Kempe does not report diffusivity as a function of vapor activity. Our study indicates that vapor activity can have a significant effect on both the mechanism of diffusion and the values measured for diffusivity and sorption.

The results of this work highlight the important role played by functional groups (whether deliberately or accidentally introduced) within a PDMS network, as was discussed previously by Baron.[11] In addition, our careful quantification of this material will assist others in assessing the moisture egress rates into devices protected by Sylgard-184, which may assist in material selection or estimating a devices lifetime in a moist environment. Most importantly, our approach serves as a rigorous method for quantifying and characterizing moisture egress into hydrophobic polymeric materials and elucidates our fundamental understanding of sorptive transport mechanisms.

ASSOCIATED CONTENT

Supporting Information

Values for the activity based sorption equation along with the activity based diffusive barriers may be found in the Supporting Information. This information is available free of charge via the Internet at http://pubs.acs.org.

AUTHOR INFORMATION

Corresponding Author

*E-mail: harley2@llnl.gov.

Notes

The authors declare no competing financial interest.

ACKNOWLEDGMENTS

The authors would like to thank Dr. Tom Wilson for preparing samples and Dr. James Lewicki for helpful discussion. This work was performed under the auspices of the U.S. Department of Energy by Lawrence Livermore National Laboratory under Contract W-7405-Eng-48 and Contract DE-AC52-07NA27344.LLNL-JRNL-559092.

REFERENCES

(1) Hillborg, H.; Gedde, U. W. *IEEE Trans. Dielectr. and Electr. Insul.* **1999**, *6*, 703−717.

(2) Kempe, M. D. *Conf. Rec. IEEE Photovoltaics Spec. Conf.* **2005**, 503−506.

(3) Fan, Z. Y.; Razavi, H.; Do, J. W.; Moriwaki, A.; Ergen, O.; Chueh, Y. L.; Leu, P. W.; Ho, J. C.; Takahashi, T.; Reichertz, L. A.; et al. *Nat. Mater.* **2009**, *8*, 648−653.

(4) Vullev, V. I.; Wan, J. D.; Heinrich, V.; Landsman, P.; Bower, P. E.; Xia, B.; Millare, B.; Jones, G. *J Am.Chem. Soc.* **2006**, *128*, 16062−16072.
(5) Thorsen, T.; Maerkl, S. J.; Quake, S. R. *Science* **2002**, *298*, 580−584.
(6) McDonald, J. C.; Whitesides, G. M. *Acc. Chem. Res.* **2002**, *35*, 491−499.
(7) Sia, S. K.; Whitesides, G. M. *Electrophoresis* **2003**, *24*, 3563−3576.
(8) Barrie, J. A.; Platt, B. *Polymer* **1963**, *4*, 303−313.
(9) Favre, E.; Schaetzel, P.; Nguygen, Q. T.; Clement, R.; Neel, J. *J. Membr. Sci.* **1994**, *92*, 169−184.
(10) Barrie, J. A.; Machin, D. *J. Macromol. Sci., Part B: Phys.* **1969**, *B 3*, 645−655.
(11) Watson, J. M.; Baron, M. G. *J. Membr. Sci.* **1996**, *110*, 47−57.
(12) Sun, C. C.; Mark, J. E. *Polymer* **1989**, *30*, 104−106.
(13) Boonstra, B. B. *Polymer* **1979**, *20*, 691−704.
(14) Stannett, V. *J. Membr. Sci.* **1978**, *3*, 97−115.
(15) Lahiff, E.; Leahy, R.; Coleman, J. N.; Blau, W. J. *Carbon* **2006**, *44*, 1525−1529.
(16) Meares, P. *J. Am. Chem. Soc.* **1954**, *76*, 3415−3422.
(17) Michaels, A. S.; Barrie, J. A.; Vieth, W. R. *J. Appl. Phys.* **1963**, *34*, 1−13.
(18) Stannett, V.; Haider, M.; Koros, W. J.; Hopfenberg, H. B. *Polym. Eng. Sci.* **1980**, *20*, 300−304.
(19) Park, G. S. *Transport Principles: Solution, Diffusion and Permeation in Polymer Membranes*; Kluwer: Dorcrecht, The Netherlands, 1986; Vol *181*, pp 1−20
(20) Mauze, G. R.; Stern, S. A. *J. Membr. Sci.* **1982**, *12*, 51−64.
(21) Detallante, V.; Langevin, D.; Chappey, C.; Metayer, M.; Mercier, R.; Pineri, M. *J. Membr. Sci.* **2001**, *190*, 227−241.
(22) Crank, J. *The Mathematics of Diffusion*; Oxford Univeristy Press: Oxford/New York, 1979; pp 49−51.
(23) *Diffusion in Polymers*; Crank, J.; Park, G. S., Eds.; Academic Press: New York, 1968; pp 10−25.
(24) Vieth, W. R.; Sladek, K. J. *J. Colloid. Sci.* **1965**, *20*, 1014−1033.
(25) Paul, D. R.; Koros, W. J. *J. Polym. Sci. B* **1976**, *14*, 675−685.
(26) Bird, B.; Stewart, W.; Lightfoot, E. *Transport Phenomena*; Wiley: New York, 2006, p 529.
(27) Bennett, K. M.; Schmainda, K. M.; Bennett, R.; Rowe, D. B.; Lu, H. B.; Hyde, J. S. *Magn. Reson. Med.* **2003**, *50*, 727−734.